Articles

School of Electrical and Electronic Engineering

2011

High Sensitivity SMS Fiber Structure Based Refractometer – Analysis and Experiment

Qiang wu
Dublin Institute of Technology, qiang.wu@dit.ie

Yuliya Semenova
Dublin Institute of Technology, yuliya.semenova@dit.ie

Pengfei Wang
Dublin Institute of Technology, pengfei.wang@dit.ie

Gerald Farrell
Dublin Institute of Technology, gerald.farrell@dit.ie

Follow this and additional works at: http://arrow.dit.ie/engscheceart

High sensitivity SMS fiber structure based refractometer – analysis and experiment

Qiang Wu,[*] Yuliya Semenova, Pengfei Wang and Gerald Farrell

*Photonics Research Centre, School of Electronic and Communications Engineering, Dublin Institute of Technology,
Kevin Street, Dublin 8, Ireland*
[*]Corresponding author: qiang.wu@dit.ie

Abstract: we have investigated the influence of multimode fiber core (MMFC) diameters and lengths on the sensitivity of an SMS fiber based refractometer. We show that the MMFC diameter has significant influence on the refractive index (RI) sensitivity but the length does not. A refractometer with a lower MMFC diameter has a higher sensitivity. Experimental investigations achieved a maximum sensitivity of 1815 nm/ RIU (refractive index unit) for a refractive index range from 1.342 to 1.437 for a refractometer with a core diameter of 80 μm. The experimental results fit well with the numerical simulation results.

OCIS codes: 060.2370, 060.2340

References and links

1. M. Han, F. W. Guo, Y. F. Lu, "Optical fiber refractometer based on cladding-mode Bragg grating", Optics Letters, vol. 35, no. 3, pp. 399-401, 2010
2. T. Guo, H. Y. Tam, P. A. Krug, J. Albert, "Reflective tilted fiber Bragg grating refractometer based on strong cladding to core recoupling", Optics Express, vol. 17, no. 7, pp. 5736-5742, 2009
3. O. Frazao, T. Martynkien, J. M. Baptista, J. L. Santos, W. Urbanczyk, J. Wojcik, "Optical refractometer based on a birefringent Bragg grating written in an H-shaped fiber", Optics Letters, vol. 34, no. 1, pp. 76-78, 2009
4. T. Allsop, R. Reeves, D. J. Webb, I. Bennion, R. Neal, "A high sensitivity refractometer based upon a long period grating Mach-Zehnder interferometer", Review of Scientific Instruments, vol. 73, no. 4, pp. 1702-1705, 2002
5. P. Wang, Y. Semenova, Q. Wu, G. Farrell, Y. Ti, J. Zheng, "Macrobending single-mode fiber-based refractometer", Applied Optics, vol. 48, no. 31, pp. 6044-6049, 2009
6. H. M. Liang, H. Miranto, N. Granqvist, J. W. Sadowski, T. Viitala, B. C. Wang, M. Yliperttula, "Surface Plasmon resonance instrument as s refractometer for liquids and ultrathin films", Senosrs and Actuators B-Chemical, vol. 149, no. 1, pp. 212-220, 2010
7. O. Frazao, P. Caldas, J. L. Santos, P. V. S. Marques, C. Turck, D. J. Lougnot, O. Soppera, "Fabry-Perot refractometer based on an end-of-fiber polymer tip", Optics Letters, vol. 34, no. 16, pp. 2474-2476, 2009
8. C. H. Chen, T. C. Tsao, J. L. Tang and W. T. Wu, "A multi-D-shaped optical fiber for refractive index sensing", Sensors, vol. 10, no. 5, pp. 4794-4804, 2010
9. Q. Wang, G. Farrell, "All fiber multimode interference based refractometer sensor: proposal and design", Optics Letters, vol. 31, no. 3, pp. 317-319, 2006
10. L. B. Soldano, E. C. M. Pennings, "Optical multi-mode interference devices based on self-imaging: principles and applications", Journal of Lightwave Technology, vol. 13, no. 4, pp. 615-627, 1995
11. Q. Wang, G. Farrell and W. Yan, "Investigation on single-mode-multimode-single-mode fiber structure", Journal of Lightwave Technology, vol. 26, no. 5, pp. 512-519, 2008
12. W. S. Mohammed, A. Mehta and E. G. Johnson, "Wavelength tunable fiber lens based on multimode interference", Journal of Lightwave Technology, vol. 22, no. 2, pp. 469-477, 2004
13. Q. Wu, Y. Semenova, A. M. Hatta, P. Wang, G. Farrell, "Bent SMS fiber structure for temperature measurement", Electronic Letters, vol. 46, no. 16, pp. 1129-1130, 2010
14. Q. Wu, A. M. Hatta, P. Wang, Y. Semenova and G. Farrell, "Use of a Bent Single SMS Fiber Structure for Simultaneous Measurement of Displacement and Temperature Sensing", IEEE Photon. Tech. Lett., vol. 23, no. 2, pp. 130-132, 2011
15. D. P. Zhou, L. Wei, W. K. Liu and J. W. Y. Lit, "Simultaneous strain and temperature measurement with fiber Bragg grating and multimode fibers using an intensity-based interrogation method", IEEE Photonics Technology Letters, vol. 21, no. 7, pp. 468-470, 2008.

16. S. M. Tripathi, A. Kumar, R. K. Varshney, et al., " Strain and Temperature Sensing Characteristics of Single-Mode-Multimode-Single-Mode Structures", Journal of Lightwave Technology, vol. 27, no. 13, pp. 2348-2356, 2009
17. Q. Wu, A. M. Hatta, Y. Semenova and G. Farrell, "Use of a SMS fiber filter for interrogating FBG strain sensors with dynamic temperature compensation", Applied Optics, vol. 48, pp. 5451-5458, 2009
18. J. E. Antonio-Lopez, J. G. Aguilar-Soto, D. A. May-Arrioja, P. LiKamWa, and J. J. Sanchez-Mondragon, "Optofluidically Tunable MMI Filter", CLEO/IQEC 2009, pp. 1-2. Baltimore, Maryland, (2009)

1. Introduction

Optical fiber based RI sensors have been studied extensively due to the advantages they offer, such as small size, immunity to electromagnetic interference, the potential for remote operation, high sensitivity, etc [1-9]. There are a number of ways to implement RI sensing, for example using a fiber Bragg grating (FBG) [1-3], long period grating [4], macro-bend singlemode fiber (SMF) [5], surface plasmon resonance [6], a Fabry-Perot interferometer [7], a multi-D-shaped optical fiber [8] or a singlemode-multimode-singlemode (SMS) fiber structure [9]. An SMS fiber structure based optical sensor has the additional advantages of low cost and ease of fabrication. The underlying operating principle of sensors based on SMS fiber structures is multimode interference excited between modes in the multimode fiber (MMF) section, which can be influenced by external perturbation [10-12]. Thus SMS fiber structures can be used as sensors for measurands such as temperature and strain [13-17]. Recently Antonio-Lopez etc proposed to use an SMS fiber structure to realize a stable optofluidically tunable fiber laser with wide tunable wavelength range of 40 nm [18]. Our previous investigations show that a specially designed SMS fiber structure can act as a RI sensor that has an estimated maximum resolution of 3.3×10^{-5} in the range of refractive indices from 1.38 to 1.45 based on an analysis using a wide-angle beam propagation method (BPM) [9]. This shows that a SMS fiber structure based refractometer is a promising technology and that it is worthwhile undertaking further investigations with the aim of optimising for the first time the key physical parameters of an SMS structure used as a refractometer in order to maximise sensitivity. In this paper a measurement technique based on wavelength monitoring is proposed for an SMS fiber structure based refractometer and a detailed analysis of such a refractometer is undertaken, taking into account the influence of two factors: multimode section fiber core diameter and length using a mode propagation analysis (MPA) method. Experimental verification is also carried out demonstrating a maximum measured sensitivity of 1815 nm/RIU.

2. Theoretical background

The configuration of an SMS fiber structure based refractometer is shown in figure 1.
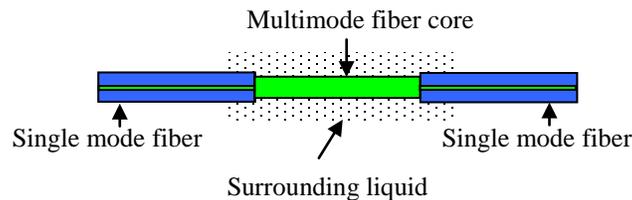

Fig. 1 Configuration of the SMS structure refractometer

In order to remove the fiber cladding and expose the multimode fiber core (MMFC) chemical etching with various chemical compounds can be used, such as Hydrofluoric acid, to controllably remove the cladding. In Fig. 1 it is clear that the surrounding liquid with an unknown RI is acting as the cladding layer to the MMFC. The light injected from the single

mode fiber (SMF) into the MMFC will excite multiple high-order modes in the MMFC. Interference between these multiple modes within the MMFC occurs and dictates the output spectral response of the SMS fiber structure, which is thus affected by the surrounding liquid RI. Assuming that the SMF and MMFC are ideally aligned, due to the circular symmetry of the input field, only LP_{0m} modes will be excited in the MMFC when light travels from SMF to MMFC. If the input light in the SMF has a fundamental mode field distribution $E(r,0)$, then the input field can be decomposed into the eigenmodes LP_{0m} in the MMFC when the light enters the MMFC section [10-12].

Defining the field profile of LP_{0m} as $\psi_m(r)$, the input field at the MMFC can be written as:

$$E(r,0) = \sum_{m=1}^{M} b_m \Psi_m(r) \qquad (1)$$

where $\psi_m(r)$ are the eigenmodes of the MMF determined by the fiber core diameters, fiber core and cladding refractive indices and where b_m is the excitation coefficient of each mode, which can be expressed as:

$$b_m = \frac{\int_0^\infty E(r,0)\Psi_m(r)rdr}{\int_0^\infty \Psi_m(r)\Psi_m(r)rdr} \qquad (2)$$

The field MMF section at a propagation distance z can thus be calculated by

$$E(r,z) = \sum_{m=1}^{M} b_m \Psi_m(r)\exp(j\beta_m z) \qquad (3)$$

where β_m is the propagation constant of each eigenmode of the MMF. The transmission power can be determined by using overlap integral method between $E(r,z)$ and the fundamental mode of the output SMF $E_0(r)$ as

$$L_s(z) = 10 \cdot \log_{10} \left(\frac{\left| \int_0^\infty E(r,z)E_0(r)rdr \right|^2}{\int_0^\infty |E(r,z)|^2 rdr \int_0^\infty |E_0(r)|^2 rdr} \right) \qquad (4)$$

As the RI of the surrounding liquid changes, the effective RI of the cladding of the fiber changes, and hence the eigenmodes $\psi_m(r)$ excited in the MMFC will change, resulting in the changes for the excitation coefficient of each mode b_m in Eq. (2) and the interference within the MMFC in Eq. (3) and the output to the SMF in Eq. (4). It is well known that MMFC diameter will influence the eigenmode $\psi_m(r)$ distribution in the MMFC section and that the MMFC length will also affect the interference between the eigenmodes $\psi_m(r)$. Both parameters will determine the final output to the SMF as shown in Eq. (4).

3. Numerical simulations

Simulations were firstly carried out with an MMFC diameter of 50 μm. To determine the optimal length of MMFC, light propagation along the MMFC was simulated using Eq. (3). Figure 2 shows the amplitude distribution of the calculated field along the MMFC. In this simulation, the MMFC and the cladding (surrounding liquid) have refractive indices of 1.4446 and 1.41 respectively.
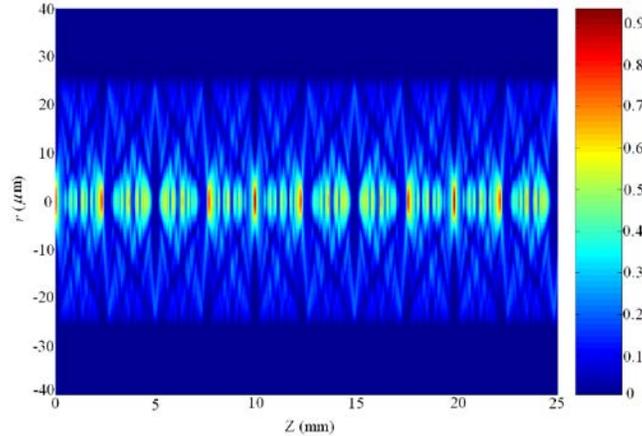
Fig. 2 Light propagation along the MMFC

In Fig. 2 the re-imaging point within the MMFC is evident at a z position circa 10 mm. To investigate the influence of the MMFC length, the first re-image (10 mm) and the second re-image (20 mm) lengths were selected for numerical simulations. The spectral responses of the refractometers with MMF section lengths of 10 and 20 mm for surrounding liquids with various refractive indices were simulated as shown in Fig. 3. In this simulation, the SMF has a core diameter of 8.3 μm and refractive indices of the core and cladding are 1.4504 and 1.4447 respectively, and the MMFC has a RI of 1.4446 and a core diameter of 50 μm.
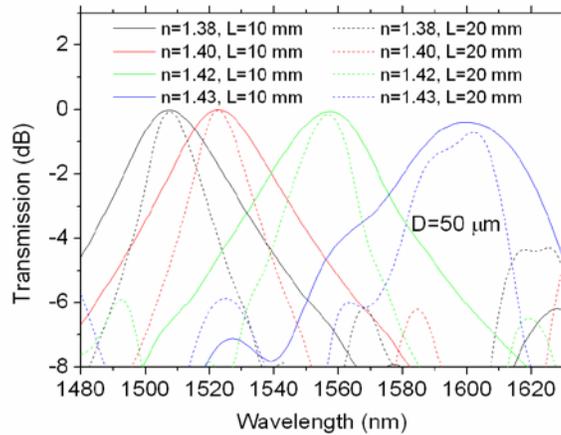

Fig. 3 Spectral response of the two SMS fiber structure based refractometers for surrounding liquids with various refractive indices

Figure 3 firstly shows that the spectral response of an SMS fiber structure is a bandpass response. As the RI increases, the central wavelength of the bandpass spectrum increases monotonically. The change in centre wavelength with RI is the same for both MMF section lengths, as expected given the periodic self-imaging occurring in the MMF section, leading to the conclusion that MMFC section length will not significantly influence the sensitivity of the refractometer. Further simulations show that the likely independence of the sensitivity of the refractometer from the MMFC section length is also observed for MMFs with different core diameters, for example 80 and 105 μm. In order to minimise the physical size of the refractometer, an MMFC section length equal the first re-image length (10 mm in Fig. 3) is chosen for further investigations of the central wavelength as a function of cladding RI. The

simulated results for central wavelength shift vs. cladding RI for different MMFC diameters of 50, 80 and 105 μm and appropriate re-imaging lengths of 10, 25 and 42 mm respectively are shown in Fig. 4. It is noted that we use 3 dB mean wavelength as central wavelength in this paper because it is a more reliable measure by comparison to peak wavelength, especially for a spectrum with a relatively flat peak response.
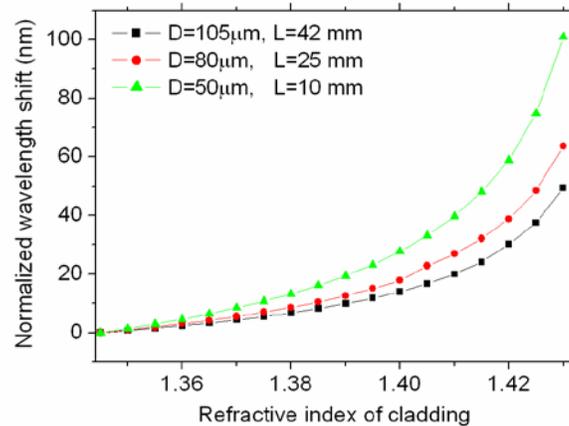

Fig. 4 Calculated central wavelength shift vs. cladding refractive index

Figure 4 firstly confirms that as the cladding (liquid) RI increases, the central wavelength of the SMS fiber structure increases monotonically for all the three MMFC diameters. The rate of increase at lower cladding (liquid) refractive indices is less than that at higher cladding refractive indices in all three cases. It can be shown from Fig. 4 that for RI range from 1.345 to 1.43, the wavelength shift of the SMS refractometer with MMFC diameter of 50 μm is larger than 100 nm which is twice of that (50 nm) for a MMFC diameter of 105 μm. The calculated sensitivities for the three cases are demonstrated in Fig. 5.
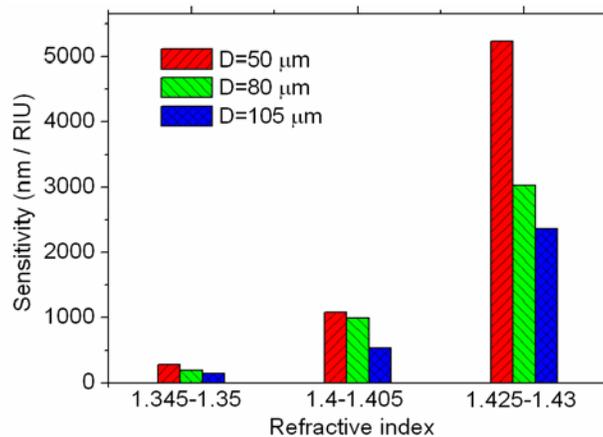

Fig. 5 Calculated sensitivity for the three cases

Figure 5 shows that the sensitivity in the RI range from 1.425 to 1.43 is larger than that in the RI range from 1.345 to 1.35 for all the three cases. Comparing the three cases, it is easy to see that there is maximum sensitivity for D = 50 μm and minimum sensitivity for D = 105 μm. An SMS fiber structure based refractometer with D=50 μm has an estimated sensitivity of 282

nm/RIU in the RI range from 1.345 to 1.35 and 5235 nm/RIU in the RI range from 1.425 to 1.43, which is higher than the corresponding sensitivity in the other two cases. This result indicates that the refractometer with a smaller MMFC diameter has a higher sensitivity. It is noted that such a refractometer may also provide a higher RI measurement range, but would require a wider bandwidth optical source. Additionally such a refractometer would also have lower RI sensitivity when the measured RI is lower than 1.345 as indicated in Fig. 4.

4. Experimental verification

To verify the analysis above, experiments were carried out using an etched SMS fiber structure. The SMS fiber structure was firstly fabricated by fusion splicing single- and multimode fibers of type SMF28 and AFS105/125Y respectively. The multimode fiber section was then immersed in an aqueous solution of hydrofluoric acid (HF, ~48%) to remove in the first instance the cladding of the AFS105/125Y multimode fiber, providing MMFC samples with a bare core with a diameter of 105 μm. A further etch stage was also used to fabricate MMFC samples with a bare core diameter of 80 μm. Further etching to achieve a bare core diameter of 50 μm was also carried out, but the samples could not be utilised experimentally as splicing joints between the SMFs and MMF failed frequently. Hence experiments were only carried out for fiber samples with bare core diameters of 105 and 80 μm. Following etching the samples were carefully cleaned firstly by a flow of de-ionised water and then by de-ionised water in an ultrasonic bath. The cleaned samples were then polished by high temperature heating at a temperature of circa 1250 ℃, which is within the glass transition temperature range of the silica material. Figure 6 shows a microscope image of the etched joint between the AFS105/125Y multimode fiber with a core diameter of 80 μm and SMF28 and its spectral response for different surrounding RI liquids.
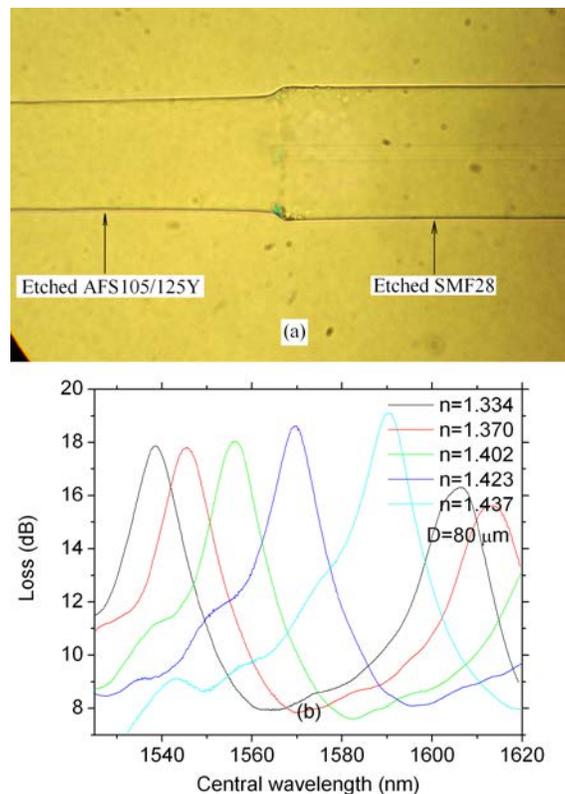
Fig. 6 (a) A microscope image of the etched joint between AFS105/125Y multimode fiber with a core diameter of 80 μm and SMF28 and (b) measured spectral response of this structure at different surrounding refractive indices

Figure 6(b) shows that as the surrounding RI increases, the central wavelength of the SMS refractometer increases monotonically. The spectral response shifts vs. different surrounding refractive indices for SMS refractometers with core diameter of 80 and 105 μm were measured and are shown in Fig. 7.
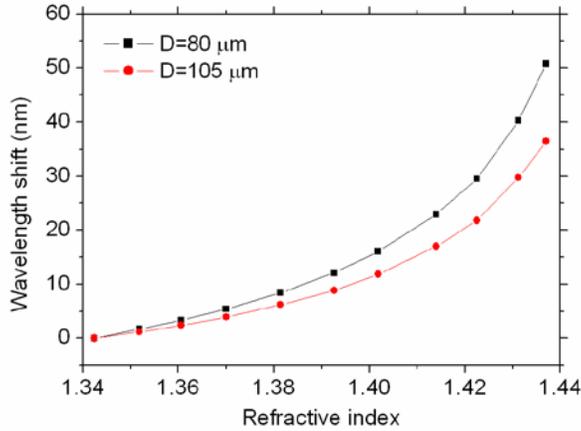

Fig. 7 Measured spectral response shifts vs. surrounding refractive index

Figure 7 shows that the rate of increase for lower liquid refractive indices is less than that at higher liquid refractive indices in both cases. Furthermore for the same RI range from 1.342 to 1.413, the wavelength shift of the SMS refractometer with a core diameter of 80 μm is larger than that with core diameter of 105 μm. By comparing Fig. 7 and Fig. 4, it is easy to see that as RI increases, the experimental wavelength shift behaviour in Fig. 7 compares very well with the simulation results in Fig. 4. The estimated sensitivities in Fig. 7 based on the measured results for both cases are shown in Fig. 8.
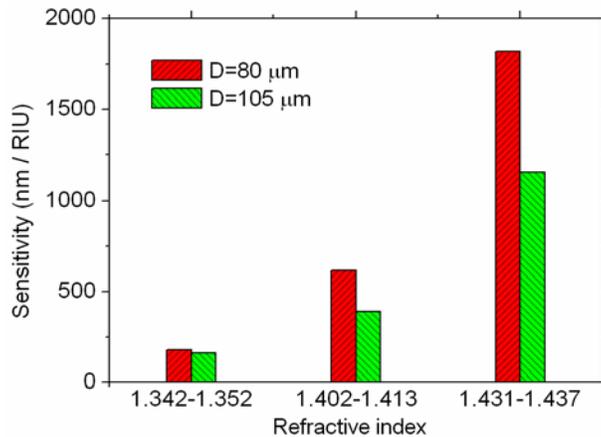

Fig. 8 Calculated sensitivities for the both cases

Figure 8 shows that the sensitivity in the RI range from 1.431 to 1.437 is larger than that in the RI range from 1.342 to 1.352 for both core diameters and the SMS refractometer with a

core diameter of 80 μm has a higher sensitivity than that with core diameter of 105 μm. The SMS fiber structure based refractometer with a core diameter of 80 μm has an estimated sensitivity of 180 nm/RIU in the RI range from 1.342 to 1.352 and 1815 nm/RIU in the RI range from 1.431 to 1.437, which is higher than the corresponding sensitivity of the refractometer with a core diameter of 105 μm. Overall the experimental results fit well with the simulation results.

Finally it is worth noting the advantage of a measurement principle based on wavelength rather than on intensity variations. The measurement principle for an SMS based refractometer used in [9] is based on monitoring power variations at a fixed wavelength. However the disadvantage of this technique is the dependence of the readings on the optical attenuation properties of the liquid under test. A simple example is that if two liquids have the same RI but different light propagation attenuation coefficients (absorption), the power measured by the technique in [9] will be different resulting in different RI readings for the two liquids. A technique based on wavelength monitoring as used in this paper can overcome this problem.

5. Conclusion

In conclusion we have analyzed the influence of MMFC diameters and lengths on the sensitivity of an SMS fiber based refractometer. The conclusion is that the MMFC length does not have a significant influence on the sensitivity of the refractometer, but the diameter influences it significantly. A higher MMFC diameter will result in a lower sensitivity. Numerical simulation results show that in the RI measurement range from 1.345 to 1.43, refractometers with MMFC diameters of 50, 80 and 105 μm have minimum estimated sensitivity of 282, 188 and 143 nm/RIU respectively and have a maximum sensitivity of 5235, 3034 and 2368 nm/RIU respectively. The refractometer with a smaller MMFC diameter has a higher sensitivity compared to that with a larger MMFC diameter. Experimental investigations verified the simulation results, achieving a maximum sensitivity of 1815 and 1156 nm/RIU in the refractive index range from 1.431 to 1.437 and minimum sensitivity of 180 and 164 nm/RIU in the refractive index range from 1.342 to 1.352 for refractometers with core diameters of 80 and 105 μm respectively. Improved sensitivity could be achieved experimentally using an MMFC of 50 μm, provided that a reliable SMF-MMF splicing technique can be perfected. Since this SMS fiber structure based refractometer has a high sensitivity, it has the potential application for bio-sensing.